Efficient ATRP Initiator/Grafting Layered Silicates: Experimental and Theoretical Investigation

D. Lerari [1, 2] [*], M. Ouraghi[1, 2], A. Benaboura[2]

[1] Centre de Recherche Scientifique et Technique en Analyses Physico-chimiques (CRAPC), BP 384, Bou-Ismail Tipaza RP 42004, Algérie

[2] Université des Sciences et de la Technologie Houari Boumediene, Faculté de Chimie, Laboratoire de Synthèse Macromoléculaire et Thio-organique Macromoléculaire, B.P 32 El-alia, 16111 Bab-ezzouar, Alger, Algeria

Abstract

An original ammonium bromide molecule, [2-(2-bromo-2-methyl-propionyloxy)-ethyl] dimethyle octadecyl ammonium bromide (OCTANBr[i]BBr), was synthesized and characterized by Fourier transform infrared spectroscopy (FTIR) and ^{1}HNMR analysis. For sake of comparison, the molecular structure, harmonic vibrational frequencies and electronic density distribution were established using density functional theory (DFT/B3LYP) with 6-31G* and 6-311G* basis set. The chemical shifts were calculated using Gauge-Independent Atomic Orbital (GIAO) method. Moreover, conformational flexibility and molecular energy profile of the compound were obtained by the same methods with respect to selected degree of torsional freedom, which was varied from - 180° to + 180°. Interestingly, the obtained results show a good agreement with the experimental ones. This synthesized molecule was evaluated in atom transfer radical polymerization (ATRP) of methyl methacrylate monomer (MMA). However, subsequent ATRP experiments of methyl methacrylate in presence of OCTANBr[i]BBr, as initiator and Cu (I) Br/1,1,4,7,10,10- hexamethyl triethylene tetramine (HMTETA) as catalysts, were afford homopolymer with predictable molecular weight and low polydispersity. Moreover, it was found to act efficiently as an organomodifier for polymer/clay nanocomposites, as was evidenced by WAXD characterizations.

1. Introduction

The dispersion of layered silicates in polymer matrix is a key to ensure some improvement in physical properties of resulted nanocomposites such as mechanical, thermal and barrier properties [1-4]. In order to optimize the compatibility between the matrix and the clay nano-platelets and overcome to the problem of dispersion, researchers are focused on the use of controlled polymerization methods. Atom Transfer Radical Polymerization (ATRP) was widely used as new reliable methodology to achieve well structural polymers. Its application is recommended for polymers which require high initiator efficiency, narrow polydispersity index (PDI) and a moderate reaction rate during the polymerization [5, 6]. Methyl methacrylate (MMA) is one of the most studied monomers for ATRP. For examples, Matyashaweski and coworkers have demonstrated the interest of using ATRP as controlled radical polymerization to prepare, in micro emulsion, stable translucent micro latex based on PMMA and PS with narrow particle size distribution [7]. Minet et al were presented the results of using ATRP as a way to synthesize brush PMMA and brush diblock PS-b-PMMA [8]. Dubois et al were interested on the efficiency of ATRP of methyl methacrylate (MMA) initiated by ethyl-2-bromoisobutyrate (EBr[i]B) and ligated on crossliked diphenyl phosphino polystyrene resins (PS-PPh$_3$/NiBr$_2$) [9]. In the aim to prepare polymer nanocomposites with controlled dispersion, we have tested the synthesized ammonium: [2-(2-

bromo-2-methyl-propionyloxy)-ethyl] dimethyle octadecyl ammonium bromide, noted: OCTANBr[i]BBr [10] as a new ATRP-initiator for methyl methacrylate monomer. With a specific aim to determine the factors governing the conformational stability of this new molecule (OCTANBr[i]BBr), we have studied and compared both theoretical and experimental methods to understand and identify the molecular interactions which can be developed. These interactions seem to play an important role to determine the conformational preferences of OCTANBr[i]BBr molecule. To the best of our knowledge, no theoretical study for this new compound has been reported. In this contribution, we describe, for the first time, the conformational behavior of OCTANBr[i]BBr and the factors that affect its stability, in absence of nanofillers, using GAUSSIAN 09W software package [11] for molecular modeling methods carried out and density functional theory (DFT) [12]. The predominant structure prompted our attention to investigate the interactions which can be developed in presence of nanofillers for polymer (nano)composite synthesis.

2. Experimental

2.1. *Materials*

Methyl methacrylate (MMA, 99% from Aldrich) was passed through a column of basic alumina (Aldrich) to remove the stabilizer (inhibitor), dried over calcium hydride (CaH_2, 98% Aldrich) for 24h and distilled under reduced pressure prior to use. Triethylamine (NEt_3, 99% from Aldrich) was dried over barium oxide (BaO, 98% Aldrich) for 24h and was distilled under reduced pressure before use. *N,N-* dimethylethanolamine (from Chem-Lab), 1-bromooctadecane (from Sigma Aldrich), 2-bromoisobutyryl bromide (98% from Aldrich), magnesium sulfate (99%, from Aldrich), sodium hydrogenocarbonate (99%, from Aldrich), copper bromide (98% from Fluka), 1,1,4,7,10,10- hexamethyltriethylenetramine (HMTETA, 97%, from Aldrich) were used as received without further purification. The Algerian clay (AC) used in this study was kindly supplied by Entreprise Nationale des Produits Miniers Non-Ferreux et des Substances Utiles (ENOF), Algeria. Its chemical composition was determined by the supplier $(Si_{4.24})^{IV}(Al_{1.24} Mg_{0.2} Fe_{0.17} Ti_{0.01})^{VI} O_{10} (OH)_2, nH_2O Na_{0.13}, Ca_{0.01}, K_{0.1}$.

2.2. *Synthesis of quaternary ammonium [2-(2-bromo-2-methyl-propionyloxy)-ethyl] dimethyle octadecyl ammonium bromide (OCTANBr[i]BBr)*

Following the procedure reported elsewhere [10], the [2-(2-bromo-2-methyl-propionyloxy)-ethyl]-dimethyl-octadecyl-ammonium bromide was synthesized by esterification reaction of synthesized alcohol: octadecyldimethyl hydroxyethyl ammonium bromide by the addition of triethylamine and an excess of 2-bromoisobutyryl bromide (Scheme 1).
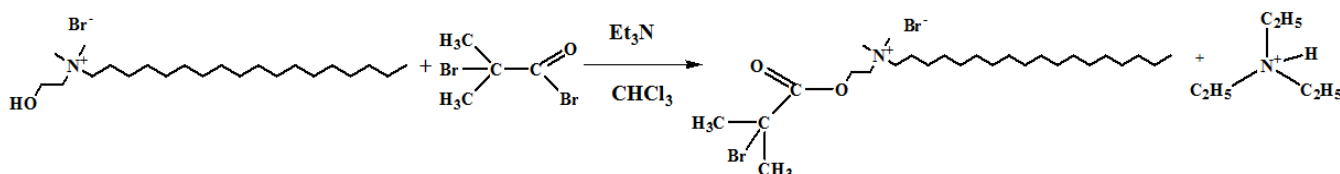
Scheme 1: Synthesis of the [2-(2-bromo-2-methyl-propionyloxy)-ethyl] dimethyle octadecyl ammonium bromide (OCTANBr[i]BBr)

2.3. *Computational details*

All molecular quantum chemical calculations were performed with the GAUSSIAN 09 program package [11]. The study of the compound was accomplished according to density functional theory (DFT) [12]. The molecular geometry optimizations and the magnetic shielding calculations were performed using Becke's hybrid functional B3LYP methods [13-16] by employing 6-31G* and 6-311G* basis set. [11, 13-16]. The results were analyzed with the Gaussview 5.0 molecular visualization program [17].

2.4. *Use of OCTANBr[i]BBr as clay organomodifier and ATRP initiator of methyl methacrylate monomer*

The organophilic form of clay was obtained by ion exchange reaction of the Na^+ cations with OCTANBr[i]BBr. The clay organomodification was preceded as follows: clay was added into water under mechanical stirrer. Then, ammonium bromide salt was added to the clay suspension. After 17 hours under stirring at 80 °C, the mixture was filtered off and the collected organomodified clay was washed with hot water to eliminate the excess of ammonium bromide (as checked by $AgNO_3$ test).

For the atom transfer radical polymerization, the catalyst was introduced in a glass tube reactor equipped with a three-way stopcock. Three nitrogen vacuum cycles were performed. Dioxane as a solvent, monomer, initiator and soluble ligand were added in a separated flask and bubbled with nitrogen before being transferred into the glass reactor by using a previously flame-dried stainless steel cannula. The mixture was subsequently heated up to the desired temperature (80°C) under magnetic stirring. Samples were withdrawn at different time intervals to determine the monomer conversion, number average molecular weight (M_n) and molecular weight distribution (M_w/M_n). The polymerization reaction was stopped by cooling down the glass tube reactor in liquid nitrogen, and after the support settling, the polymer solution was removed under a slight nitrogen overpressure via a stainless steel cannula. The catalytic support was washed with extra solvent and dried under vacuum while the polymer solution was poured into an excess volume of heptane. The as-recovered polymer was obtained after precipitation, filtration and drying under reduced pressure [10]. Scheme 2 illustrates the proposed mechanism.
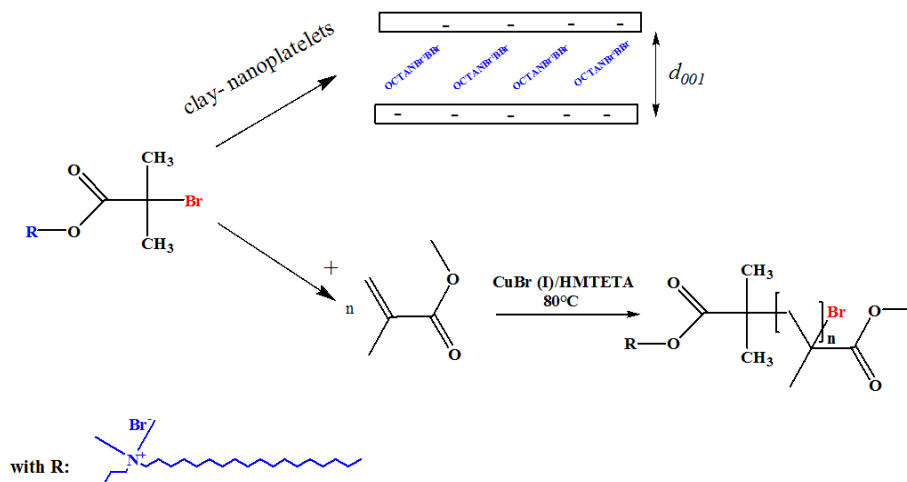
Scheme 2: General mechanism of (a) organomodification of montmorillonite nanoplatelets in presence of OCTANBr^{i}BBr as organomodifier, (b) ATRP of MMA in presence of OCTANBr^{i}BBr as initiator.

2.5. *Characterization*

FTIR measurements were performed on a Bruker spectrometer at resolution of 32 cm^{-1} and scan number of 64. ^{1}H NMR spectra were recorded on a 300 MHz Bruker spectrometer using TMS as reference. Molecular weights and molecular weight distributions were measured in THF at 35°C using size exclusion chromatography (SEC) on a Polymer Lab system equipped with a Basic-Marathon Autosampler, a guard column (PLgel 10 μm 50 x 5mm), two mixed-B columns (PLgel 10μm 300 x 7.5mm), and a differential refractive index detector (PL-RI). Molecular weights were calibrated using linear PMMA standards in the range of 600–1 700.000 g.mol^{-1}. XRD patterns were recorded on a Siemens D5000 diffractometer with the Cu K_α radiation (λ=0.15406 nm) from 1.65° to 30° by step of 0.04° and scanning rate of 10°/min; under the accelerating voltage of 40 kV .

3. Results and discussion

3.1. *Spectroscopy*

The OCTANBr^{i}BBr was first characterized by FTIR analysis. As illustrate in (figure 1a), FTIR spectra show especially, the disappearance of the OH band at 3340 cm^{-1} and 3240 cm^{-1} attributed to the elongation vibrations of hydroxyl-terminated OCTANBrOH molecule and the appearance of the C=O band at 1740 cm^{-1}. On the other hand, the computed harmonic vibrational frequencies were identified. A shown in Table 1, the C=O stretching vibrations were observed at 1799 cm^{-1}/1789 cm^{-1} and the C-O-C asymmetrical stretching at 1161 cm^{-1}/1182 cm^{-1}. Symmetric and asymmetric C-H stretching vibrations were identified in the range of 3010 cm^{-1}/ 3395 cm^{-1}. C-N stretching vibrations were noticed at 1244 -1242cm^{-1}. Clearly, the experimental and calculated frequencies show slight differences. The first reason is that the experimental spectrum was recorded for the compound in the solid state, while the computed spectra correspond to isolated molecule in the gas phase. The second reason is the fact that the experimental values correspond to inharmonic vibrations, whereas the calculated values correspond to harmonic ones [18]. Despite the differences between observed and calculated values, the general agreement is good.
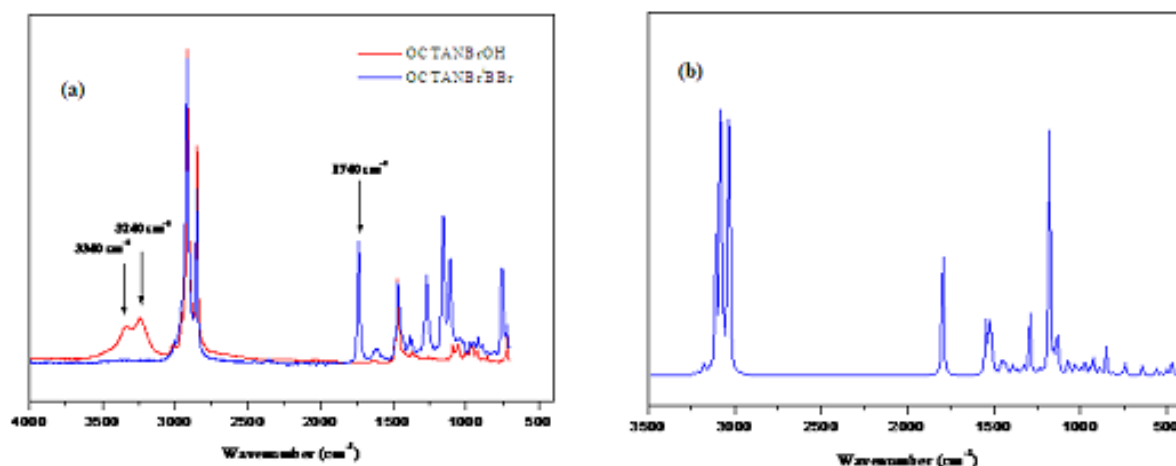
Figure1: Experimental FTIR spectra of OCTANBrOH and the resulting OCTANBr[i]BBr (a) and predicted spectrum by DFT/B3LYP (b).

Table 1: Vibrational frequency modes (cm^{-1}) obtained from experimental and theoretical calculations at B3LYP/6-31G* and B3LYP/6-311G*. **(a)**

Assignment	Frequencies		
	Experimental	B3LYP/6-311G*	B3LYP/6-31G*
Ester (C=O) stretch	1737	1789	1799
C-O-C asymmetrical stretching	1157	1161	1182
asymmetric stretching of CH$_3$	2916	3123-3196	3138-3238
symmetric stretching of CH$_3$	-	3091-3104	3100-3122
asymmetric stretching of CH$_2$	2850	3026-3047	3030-3054
symmetric stretching of CH$_2$	-	3000-3022	3010-3030
C-N-C scissor	1269	1242	1244

^{1}H NMR spectra confirm the quantitative reaction of the hydroxyl end-groups to the carbonyl ones, as evidenced by the presence of the sharp signal at about 1.95 ppm assigned to the OC-C-CH$_3$ protons of the OCTANBr[i]BBr and the quantitative shift of the signals at 3.76 ppm and 4.13 ppm in favor of new resonances centered at 4.22 ppm and 4.69 ppm, respectively (Figure 2). It is believed that ^{1}H chemical shifts can be accurately determined by the Gauge Including Atomic Orbital (GIAO) method at B3LYP/6-31G* and B3LYP/6-311G* levels [19,20]. We adopt this method to calculate the chemical shielding constants by using a key word ''NMR = GIAO'' in GAUSSIAN 09. In order to compare isotropic shielding with experimental chemical shifts, the ^{1}HNMR parameters for the reference molecule tetramethylsilane (TMS) were considered [21]. So, in order to express the chemical shifts in ppm, the geometry of the tetramethylsilane (TMS) molecule was optimized and then its ^{1}HNMR spectrum was calculated by using the same method and basis set. The calculated isotropic shielding constant σ_i was then transformed into chemical shifts relative to TMS by $\delta = \sigma_{TMS} - \sigma_i$. For reliable assignments of ^{1}HNMR spectra, our experimental investigations are compared with theoretical calculations. The results are in perfect accordance, as shown in table 2.

3.2. Relative energies and structure of the OCTANBr[i]BBr conformers

In order to predict the most stable geometry of the studied molecule, potential energy scan (PES) was performed using B3LYP/6-31G* level of theory. In first, scan profile of the aliphatic part about the dihedral angle C_n-C_{n+1}-C_{n+2}-C_{n+3} were explored from -180° to 180° of 5°, with relaxing all other geometrical parameters during the scan. Figure 3 represents PES scan profile of following dihedral angle C_1-C_2-C_3-C_4, C_5-C_6-C_7-C_8, C_9-C_{10}-C_{11}-C_{12} and C_{13}-C_{14}-C_{15}-C_{16} respectively. Their corresponding conformations are presented in figure 4.
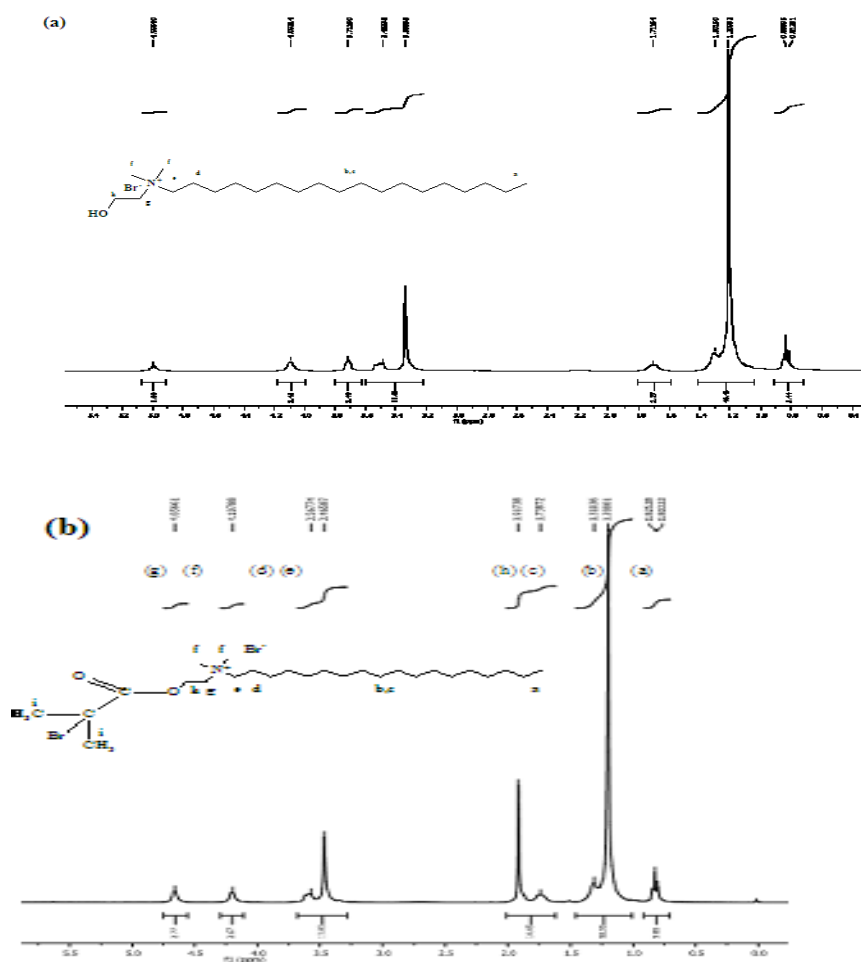
Figure2: ^{1}H NMR spectra of OCTANBrOH (a) and the resulting OCTANBr^{i}BBr (b).

Table 2: Theoretical and experimental ^{1}H isotropic chemical shifts (δ_{iso}) (with respect to TMS all values in ppm) for the title compound.

Atom	Experimental	B3LYP/6-311G*	B3LYP/6-31G*
Ha	0.86	0.65	0.66
Hb	1.24	1.20	1.28
Hc	1.78	2.10	3.49
Hd	1.95	1.92	2.02
He	3.49	3.27	3.07
Hf	3.63	2.83	2.65
Hg	4.22	3.78	3.17
Hh	4.69	4.16	3.95

All profiles PES scan reveal one stable conformer represented with ground state energy (-3799.42840397 Hartree). As a second step, further scan were performed by varying dihedral angles N-C-C-C and -O-C-C-N- respectively. Corresponding PES profiles scan are illustrated in figures 5 and 6. The angles values of the N-C-C-C bond is equal to 9.47° for the stable form and 180.0° in the less stable one (Figure 5). In the case of O-C-C-N bond, this angle is equal to -87,03° for the stable form and -2.03° for the less stable one (Figure 6). Selected bond distances, angles and dihedral angles for different forms are listed in table 3. The optimized structures of the studied conformers show that the bond distances C—Br:2.03 Å, -C—NH$_2$-: 1.53 Å and –N—CH$_3$: 1.51 Å are higher in stable form than that other forms whereas bond distances –C—O-: 1.35 Å, –C=O:1.21 Å and bond angles –C—C—Br:107.47° , -C—C=O:124.77° , -C—O—C-: 117.36°are lower in stable form than that other forms. So, the dihedral angles Br—C—C=O: 102.79° and –N—C—C—C-: 177.12° are higher in stable form.
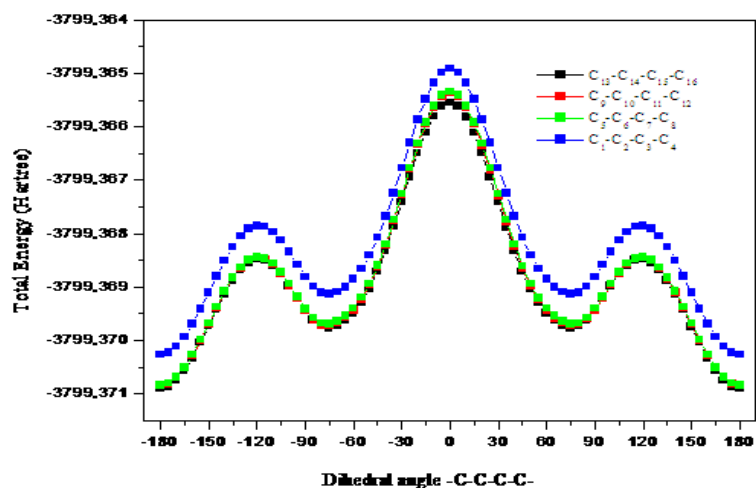
Figure3: Energy curves for conformers a, b, c and d along dihedral angle –C-C-C-C- calculated at B3LYP/6-311 G*.

Form (a)

Form (b)

Form (c)

Form (d)
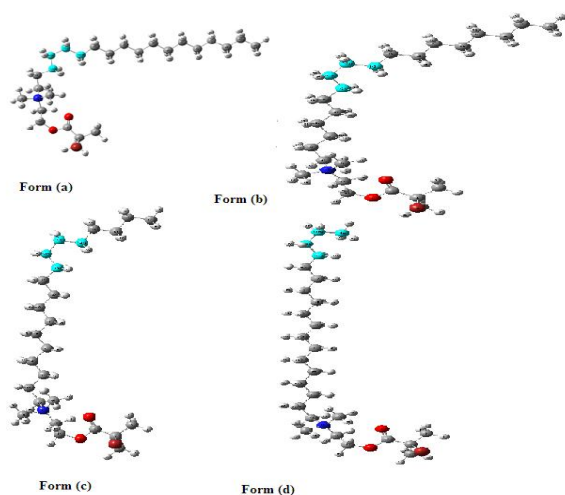
Figure4: Probable conformers of OCTANBr[i]BBr.
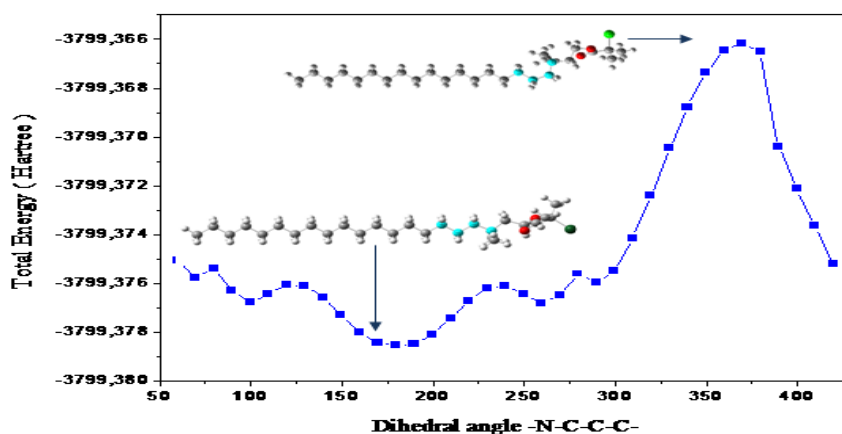
Figure5: Energy curve for conformer E along dihedral angle –N-C-C-C calculated at B3LYP/6-31 G*.

According to these results, the geometrical structure corresponding to the lowest minima in the potential energy surface is presented in figure 7. Its total energy, dipole moment, charge of Mullikan HOMO and LUMO are summarized in table 4. Figure 7 illustrates this optimized structure based on charge of Mullikan HOMO and LUMO.
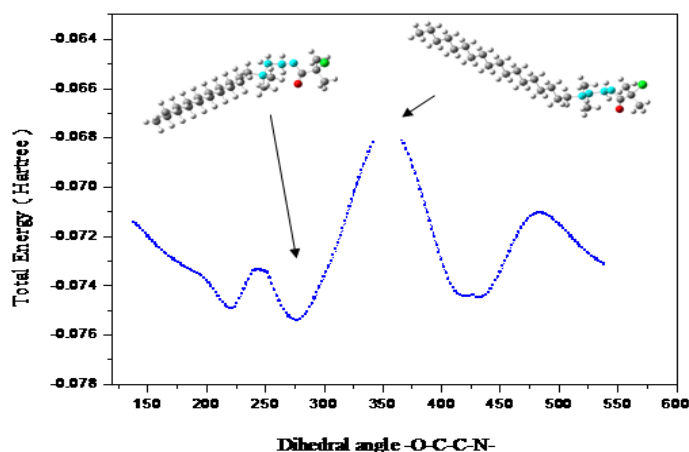
Figure6: Energy curve for conformer F along dihedral angle –O-C-C-N calculated at B3LYP/6-31 G*.

(a)

(b)
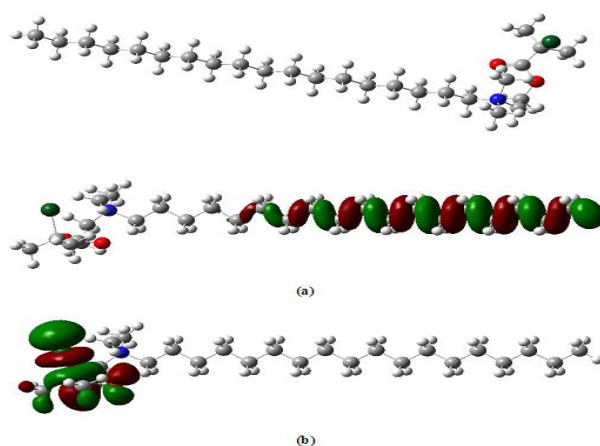
Figure7: Optimized stable form of OCTANBr^iBBr: ○ Hydrogen; ● Carbon; ● Oxygen; ● Nitrogen; ● Bromide Frontier molecular orbitals. The highest occupied molecular orbital (HOMO) (a) and the lowest un-occupied molecular orbital (LUMO) (b) for the stable form of OCTANBr^iBBr**.**

Table 3: The geometric parameters of bond lengths (Å), bond angles and selected dihedral angles (°).

	Form a	Form b	Form c	Form d	Form e	Form f	Stable Form
Bond length							
-C—Br	1.96	1.96	1.96	1.96	1.96	1.96	2.03
-C—O-	1.37	1.37	1.37	1.37	1.37	1.38	1.35
-C=O	1.23	1.23	1.23	1.23	1.23	1.22	1.21
-N—CH2-	1.51	1.51	1.51	1.51	1.51	1.51	1.53
-N—CH3-	1.49	1.49	1.49	1.49	1.49	1.49	1.51
Bond angle							
-C—C—Br	109.92	109.92	109.92	109.92	109.92	109.89	107.47
-C—C=O	129.44	129.44	129.44	129.44	129.37	129.71	124.77
-C—O—C-	117.43	117.43	117.43	117.43	117.47	118.09	117.36
-C—N—C-	109.86	109.86	109.86	109.86	110.63	110.40	109.96
-C—C—C-	111.25	111.27	111.15	111.18	111.17	111.23	113.56
Dihedral angle							
Br—C—C=O	90.55	90.55	90.54	90.54	91.00	95.24	102.79
-O—C—C—N-	-139.26	-139.25	-139.25	-139.25	-150.16	-7.03	74.42
-N—C—C—C-	99.35	99.19	99.20	99.20	9.47	101.24	177.12

3.3. *Efficiency of OCTANBr^{i}BBr as an ATRP initiator and clay organomodifier*

The studied molecule was tested as initiator for controlled polymerization of methyl methacrylate monomer. The polymerization reaction was carried out in dioxane at 80°C, using CuBr/HMTETA as catalyst. The control over the molecular parameters is generally good in terms of molar weight as well as in terms of polydispersity indices, as illustrated in figure 8. Moreover, SEC analysis shows a unimodal molecular weight distribution (Figure 9). These molecular parameters (Table5) are sufficient to confirm the efficiency of OCTANBr^{i}BBr as initiator [9]. Interestingly, the XRD spectrum related to the intercalation of this molecule on nano-clay platelets (figure 10) shows an important shift of *d*-spacing to about 43Å. This increase in interlayer spacing can promote better controlled grafting of PMMA leading to nanocomposites with finest dispersion

Table 4: Calculated parameters of the optimized structure.

	Total energy (Hartree)(thermal) E_{total} (kcal mol^{-1})	Dipole moment (Deby)	Charge of Mulliken N O (ester),(carbonyl) Br	HOMO (a.u)	LUMO (a.u)	Gap ΔE (eV)
Form a	-3799.3655432	24.5582	-0.354586 -0.457075 -0.498005 -0.052755	-0.31873	0.15432	4.4738
Form b	3799.3653669	23.7525	-0.354476 -0.456938 -0.497973 -0.052667	-0.31920	-0.15445	4.4831
Form c	-3799.36534	24.7620	-0.354343 -0.456993 -0.498080 -0.052652	-0.32478	-0.15444	4.6352
Form d	-3799.3649132	25.7274	-0.354499 -0.456973 -0.498027 -0.052655	-0.31593	-0.15443	3.9101
Form e	-3799.3614661	22.6901	-0.324526 -0.457676 -0.493046 -0.053097	-0.31429	-0.15263	4.3989
Form f	-3799.365065	22.7664	-0.342038 -0.490514 -0.457616 -0.043972	-0.31408	-0.15965	4.2023
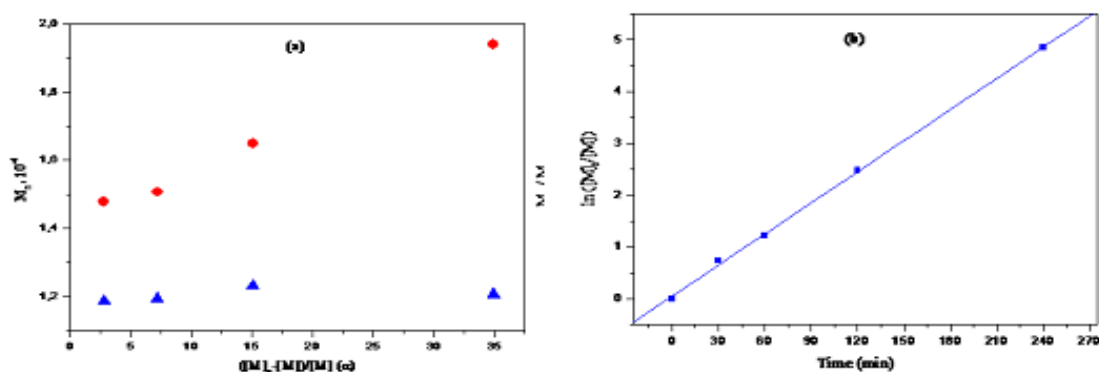
Figure8: Dependence of M$_n$ (open symbols) and M$_w$/M$_n$ (filled symbols) vs percent conversion (a) and Kinetic plot of monomer conversion for the MMA polymerization at 80°C (b).
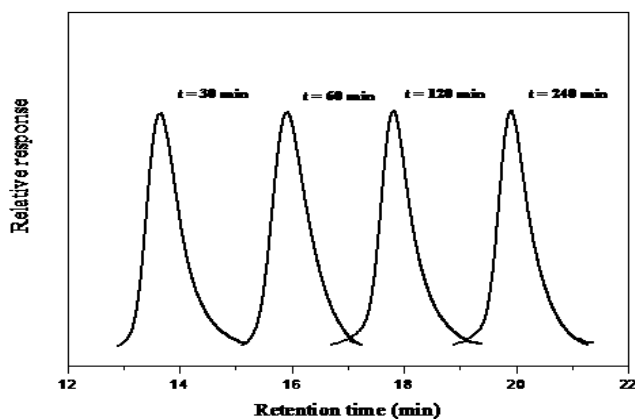
Figure9: SEC traces of PMMA formed at different reaction times.

Table 5: Molecular parameters of synthesized PMMA

Enter	t(min)	Rdt[a] (%)	$M_n^{[b]}$ 10^{-4} g.mol^{-1}	$M_w 10^{-4}$ (g.mol^{-1})	$M_w/M_n^{[b]}$	α
1	30	11.5	1.649	2.032	1.232	0.40
2	60	20	1.401	2.342	1.207	0.33
3	120	75	1.4782	1.7549	1.187	0.72
4	240	92	1.5068	1.8002	1.194	3.62

$[MMA]_0 = 2.0$ mol.L^{-1}, Toluene, 80°C, $[MMA]_0/[Br]_0$: 40, CuBr : HMTETA : 1:2.
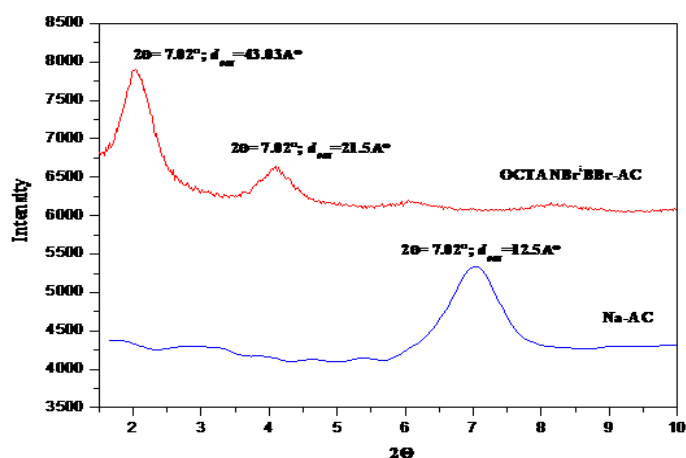
Figure10: XRD patterns of (a) Na-AC and (b) OCTANBr^{i}BBr-AC montmorillonite samples.

Conclusion

In this contribution, we have presented theoretical study of a novel synthesized ammonium acting as organomodifier of clay and initiator for ATRP of MMA: [2-(2-bromo-2-methyl-propionyloxy)-ethyl] dimethyle octadecyl ammonium bromide (OCTANBr^{i}BBr). Theoretical calculations were performed to obtain the optimized structure using electron density distribution. The obtained results were in good concordance with the FTIR and ^{1}HNMR experimental data. The polymerization of methyl methacrylate monomer (MMA) in presence of OCTANBr^{i}BBr lead to polymer with controlled composition, narrow molecular weight distribution and absence of oligomers formation. These results attest the efficient of OCTANBr^{i}BBr as ATRP initiator. This organomodifier-ATRP initiator molecule presents real interest for the controlled synthesis of polymer nanocomposites. However, it can promote more compatibility between the organomodified nanoplatelets and the polymeric matrix for reaching nanocomposites with better delamination. Such an approach is under current investigation by using ATRP of PMMA in presence of nanoclay.

References

1. Sahoo P.K., Samal R., *Polym. Degrad. Stab.* 92 (2007) 1883.
2. Wang G.A., Wang C.C., Chen C.Y., *Polym. Degrad. Stab.* 91(2006) 2443
3. Alexandre M., Dubois Ph., *Mater.Sci .Eng.* 28 (2000) 1.
4. Okamoto M., Morita S., Taguchi H., Kim Y.H., Kotaka T., Tateyama H., *Polymer* 41(2000) 3887.
5. Matyjaszewski K., *American.Chem.Soc.* 768 (2014) 136.
6. Matyjaszewski K., Xia J., *Chem. Rev.* 101 (2001) 2921.
7. Min K., Matyjaszewski K., *Macromolecules.*38 (2005) 8131.
8. Minet I., Delhalle J., Hevesi L., Mekhalif Z., *J.Coll.Inter.Sci.*332 (2009) 317.
9. Duquesne E., Habimana J., Dege´e P., Dubois P., *Chem.Commun*. (2004) 640.
10. Lerari D., Peeterbroeck S., Benali S., Benaboura A., Dubois Ph., *J.Appl. Polym.Sci.*121 (2011)1355.
11. Frisch M. J., Trucks G. W., Schlegel H. B., Scuseria G. E., Robb M. A., Cheeseman J. R., Scalmani G., Barone V., Mennucci B., Petersson G. A., Nakatsuji H., Caricato M., Li X., Hratchian H. P., Izmaylov A. F., Bloino J., Zheng G., Sonnenberg J. L., Hada M., Ehara M., Toyota K., Fukuda R., Hasegawa J., Ishida M., Nakajima T., Honda Y., Kitao O., Nakai H., Vreven T., Montgomery J. A. Jr., Peralta J. E., Ogliaro F., Bearpark M., Heyd J. J., Brothers E., Kudin K. N., Staroverov V. N., Kobayashi R., Normand J., Raghavachari K., Rendell A., Burant J. C., Iyengar S. S., Tomasi J., Cossi M., Rega N., Millam N. J., Klene M., Knox.J. E., Cross. J. B., Bakken V., Adamo C., Jaramillo J., Gomperts R., Stratmann R. E., Yazyev O., Austin. A. J., Cammi R., Pomelli C., Ochterski J. W., Martin R. L., Morokuma K., Zakrzewski V. G., Voth G. A., Salvador P., Dannenberg J. J., Dapprich S., Daniels A. D., Farkas O., Foresman J. B., Ortiz J. V., Cioslowski J., Fox D. J., Gaussian 09, Revision A.1, Gaussian: Wallingford, CT, (2009).
12. Becke A.D., *Phys. Rev.* A 38 (1988) 3098.
13. Lee C., Yang W., Parr R.G., *Phys. Rev.* B37 (1998) 785.
14. Becke A.D., *J. Chem. Phys.* 98 (1993) 5648.
15. Miehlich B., Savin A., Stoll H., Preuss H., *Chem. Phys. Lett.*157 (1989) 200.
16. Dewar M.J.S., Zoebish E.G., Healy E.F., Stewart J.J.P., *J. Am. Chem.Soc*. 107 (1985) 902.
17. Frisch E., Hratchian H.P., Dennington II. R.D., Keith T.A., Millam J., Nielsen B., Holder A.J., Hiscocks J., *Gaussian Inc, GaussView Version 5.0.8,* (2009).
18. Kowalczyk I., Bartoszak-Adamska E., Jaskolski M., Dega-Szafran Z., Szafran M., *J. Mol. Struct.* 976 (2010) 119.
19. Helgaker T., Jaszunski M., Ruud K., *Chem. Rev.* 103 (1999) 8288.
20. Wolinski K., Hinton J. F., Pulay P. J., *J. Am. Chem. Soc*. 112 (1990) 8251.
21. Rappé A.K., Casewit C.J., Colwell K.S., Goddard W.A.I.I.I., Skiff W.M., *J. Am. Chem. Soc.,* 114 (1992)10024.

(2017) ; http://www.jmaterenvironsci.com